In addition, the lines in Fig. 3(b) are observed to be a true subset of the ones in Fig. 2(b). In other words we suggest that our luminescence spectrum is due to the emission of Dy^{+3} ions in sites of one-(lower than cubic) point symmetry. This means that in accordance with our previous[2] suggestions, sites of different symmetries can be responsible for thermoluminescence emission even at temperatures close to that of liquid nitrogen. Attempts to excite luminescence of Dy^{+3} in sites of cubic symmetry only were not conclusive due to the very low intensity of the emission involved.

†Work supported by the National Research Council and Defence Research Board of Canada.

*Holder of a Province of Ontario Graduate Fellowship.

[1]M. Schlesinger and P. W. Whippey, Phys. Rev. 162, 286 (1967).

[2]M. Schlesinger and M. Nerenberg, Phys. Rev. 178, 568 (1969).

[3]Crystals from a different source (Optovac) were used also. Essentially identical results to those from the Harshaw samples were obtained from these crystals.

[4]A detailed description of the spectrograph which was constructed in our laboratory can be secured by writing to one of us (M. S.).

[5]G. H. Dieke, *Spectra and Energy Levels of Rare Earth Ions in Crystals* (Interscience, New York, 1968), pp. 268–279.

[6]Reference 5, p. 142.

[7]Z. Kiss and D. L. Staebler, Phys. Rev. Letters 14, 691 (1965).

[8]J. L. Merz and P. S. Pershan, Phys. Rev. 162, 217 (1967).

PHYSICAL REVIEW B VOLUME 3, NUMBER 9 1 MAY 1971

Electron Paramagnetic Resonance of Several Rare-Earth Impurities in the Cubic Perovskite $KMgF_3$†

M. M. Abraham, C. B. Finch,* J. L. Kolopus, and J. T. Lewis‡
Solid State Division, Oak Ridge National Laboratory, Oak Ridge, Tennessee 37830
(Received 23 November 1970)

The electron paramagnetic resonance spectra of doped $KMgF_3$ single crystals containing Yb^{3+}, Tm^{2+}, Er^{3+}, Dy^{3+}, and Gd^{3+} have been observed at 9 GHz. Cubic symmetry sites have been identified for these ions and the data indicate that the Yb^{3+}, Tm^{2+}, Er^{3+}, and Dy^{3+} substitute for the sixfold-coordinated Mg^{2+} ion, but that the gadolinium probably substitutes for a twelvefold-coordinated K^{1+} ion. Noncubic symmetry sites were also observed for Yb^{3+}, Er^{3+}, and Gd^{3+}. Hyperfine structure for the isotopes ^{171}Yb, ^{173}Yb, ^{169}Tm, ^{167}Er, ^{161}Dy, and ^{163}Dy was identified, and in some cases superhyperfine interactions with the fluorine ligand ions were observed with good resolution.

INTRODUCTION

It is well known that the fourth-order term in the expansion of the crystal-field potential has a different sign for sixfold cubic coordination as opposed to fourfold, eightfold, or twelvefold cubic coordinations.[1] For twelvefold coordinations, the sixth-order term has a different sign than for the other three types of coordination. These sign reversals lead to a different ground state for a substitutional paramagnetic impurity in sixfold coordinations than for the same ion in the other coordinations. An electron paramagnetic resonance (EPR) study of a particular rare-earth impurity ion in cubic crystalline environments with different coordinations would therefore enable different ground-state resonances to be observed for this ion. The cubic perovskite structure of $KMgF_3$ ($a_0 = 3.973$ Å) is ideal for a study of this nature.[2] The structure may be visualized as K^{1+} ions at the corners of a cube with a Mg^{2+} ion at the body center and F^- ions at the face-center positions. The Mg^{2+} ion has six F^- nearest neighbors along ⟨100⟩ directions, while the K^{1+} ion has twelve F^- nearest neighbors along ⟨110⟩ directions. Assuming that the necessary charge compensation does not occur nearby, a rare-earth ion residing in a magnesium site would experience a sixfold-coordinated cubic crystal field; if the potassium site were occupied, the cubic field would be twelvefold coordinated. The EPR spectrum obtained for the rare-earth impurity should clearly distinguish between these two types of cubic coordination. Further, any observed superhyperfine interactions with the fluorine ligand ions would be an additional aid in determining the impurity site location. Although the $4f$ electronic wave functions are fairly well localized, superhyperfine structure has been observed in the eightfold-coordinated fluorite structure of CaF_2 for $Ce^{3+}(4f^1)$,[3] $Tb^{3+}(4f^8)$,[4] $Tm^{2+}(4f^{13})$,[5] and $Yb^{3+}(4f^{13})$.[6] Superhyperfine structure has also been seen for Gd^{3+} in CaF_2 crystals that have been subjected to strains.[7] Accordingly, we have doped $KMgF_3$ single crystals with Yb^{3+}, Tm^{2+}, Er^{3+}, Dy^{3+}, and Gd^{3+} and observed the

EPR spectrum for each of these ions in cubic symmetry sites and for Yb^{3+}, Er^{3+}, and Gd^{3+} in noncubic symmetry sites as well. Hyperfine structure for the isotopes ^{171}Yb, ^{173}Yb, ^{169}Tm, ^{167}Er, ^{163}Dy, and ^{161}Dy was also identified, and in some cases superhyperfine interactions with the fluorine ligands were observed with good resolution.

THEORY

For rare-earth ions, the interaction with the crystalline electric field is very much weaker than the spin-orbit coupling. The crystal field is considered as a perturbation on the $2J+1$ degeneracy of the free-ion ground state and will partially remove this degeneracy, depending on its strength and symmetry.

In the "operator-equivalent" technique developed by Stevens, [8] the crystalline electric field is expanded in a power series, and successive terms in the expansion are replaced by suitable angular-momentum operators allowing for the noncommutation of J_x, J_y, and J_z. A good description of this method may be found in Hutchings's work, [9] where the various polynomial operators O_l^m are enumerated. The potential for cubic symmetry may be written as $\mathcal{H} = B_4(O_4^0 + 5O_4^4) + B_6(O_6^0 - 21O_6^4)$. The coefficients B_4 and B_6 are factors which determine the strength of the field. In the point-charge model, B_n is proportional to $\langle r^n\rangle/R^{n+1}$, where $\langle r^n\rangle$ is the mean nth power of the radii for the $4f$ electrons and R is the distance of the coordinating charges from the magnetic ion. The proportionality constant not only depends on the type of coordination, but also includes the operator-equivalent factor which is different for each rare-earth ion and depends on the particular J manifold.

Lea, Leask, and Wolf [10] (LLW) have performed a detailed calculation of the eigenfunctions and eigenvalues of the sublevels for all J manifolds in a cubic crystal field from $J=2$ to $J=8$. The eigenfunctions and eigenvalues with a scale factor W are tabulated as functions of a variable x, defined by

$$\frac{B_4}{B_6} = \frac{x}{1-|x|}\,\frac{F(6)}{F(4)}, \tag{1}$$

where $F(4)$ and $F(6)$ are factors common to all the matrix elements of the fourth- and sixth-order angular-momentum operators, respectively, and x varies between 0 and ± 1 (see Fig. 1).

Although the value of x (and B_4/B_6) is theoretically uncertain, the predicted sign of x does not, in practice, differ from the experimental sign. Thus, the theory allows the identification of the lowest sublevels of a particular J manifold. Some ambiguity is still present since the actual value of x is not theoretically known. The experimental data can be used to set limits on the range of x and in some cases actually to calculate the value of x directly.

Yb^{3+} and Tm^{2+}

The electronic configuration of Yb^{3+} and Tm^{2+} is $4f^{13}$ with a free-ion ground state of $^2F_{7/2}$. A cubic crystal field will split the eightfold ground-state degeneracy into a pair of doublets, Γ_6 and Γ_7, and a quartet, Γ_8. In a site for which the nearest-neighbor coordination is sixfold, the LLW parameter x is negative, W is positive, and the predicted ground state is the Γ_6 doublet, regardless of the value of x. For twelvefold cubic coordination, x is still negative, but W is reversed in sign and is negative. The predicted ground state will be either a Γ_7 doublet or a Γ_8 quartet. The Γ_6 and Γ_7 doublets will have isotropic spectroscopic splitting factors in an applied magnetic field given by $g_{\Gamma_6} = \frac{7}{3} g_{\text{Landé}}$ and $g_{\Gamma_7} = 3 g_{\text{Landé}}$. Using $g_{\text{Landé}} = 1.141\,22$, [11] the predicted g values are found to be $g_{\Gamma_6} = 2.6628$ and $g_{\Gamma_7} = 3.4237$. The splitting of the Γ_8 quartet will depend upon orientation of the applied magnetic field with respect to the crystal axes. [12]

Er^{3+}

Trivalent erbium has a $4f^{11}$ electronic configuration and a free-ion ground state of $^4I_{15/2}$. The sixteenfold ground-state degeneracy will be split by a cubic crystal field into three Γ_8 quartets and a pair of doublets, Γ_6 and Γ_7. For sixfold cubic coordination, the LLW parameter x is positive, W is positive, and either a Γ_7 doublet or a Γ_8 quartet is predicted to be lowest. For twelvefold coordination, x is still positive, but W is negative, and the ground state will be either a Γ_6 doublet or a Γ_8 quartet. The isotropic g values for the doublets will be

$$g_{\Gamma_7} = \tfrac{17}{3} g_{\text{Landé}} \quad \text{and} \quad g_{\Gamma_6} = 5 g_{\text{Landé}}.$$

Using $g_{\text{Landé}} = 1.195\,15$, [13] the predicted g values are found to be $g_{\Gamma_7} = 6.7717$ and $g_{\Gamma_6} = 5.9758$. For re-

Cubic Crystal Field Hamiltonian

$$\mathcal{H} = B_4(O_4^0 + 5\,O_4^4) + B_6(O_6^0 - 21\,O_6^4)$$

$$= B_4\,\frac{F(4)}{F(4)}\,O_4 + B_6\,\frac{F(6)}{F(6)}\,O_6,$$

$$O_4 = (O_4^0 + 5\,O_4^4), \quad O_6 = O_6^0 - 21\,O_6^4.$$

F(4) and F(6) are factors common to all the matrix elements

$$\mathcal{H} = Wx\,\frac{O_4}{F(4)} + W(1-|x|)\,\frac{O_6}{F(6)},$$

$$Wx = B_4\,F(4), \quad W(1-|x|) = B_6\,F(6),$$

$$\frac{x}{1-|x|} = \frac{B_4\,F(4)}{B_6\,F(6)}.$$

FIG. 1. Hamiltonian for cubic crystal field. The O's are operators whose transformation properties are similar to spherical harmonics. The B's determine the strength of the crystal field. For $J=\frac{7}{2}$, $F(4)=60$, $F(6)=1260$, so that $21x/(1-|x|)=B_4/B_6$. For $J=\frac{15}{2}$, $F(4)=60$, $F(6)=13\,860$, so that $231x/(1-|x|)=B_4/B_6$.

peated irreducible representations, the eigenvectors depend on the particular value of x, and therefore the experimentally observed Zeeman splitting of the Γ_8 quartet will determine the value of x.

Dy^{3+}

Trivalent dysprosium has a $4f^9$ configuration and a free-ion ground state of $^6H_{15/2}$. The situation is similar to the case of trivalent erbium with the exception that the operator-equivalent factor contained in B_4 is changed in sign and that $g_{\text{Landé}}$ is different. Therefore for sixfold coordination, x will be negative, W will be positive, and the ground state will be either a Γ_7 doublet or a Γ_6 doublet. For twelvefold coordination, x will still be negative, but W will be negative, and the resulting ground state will be a Γ_8 quartet. With $g_{\text{Landé}} = 1.3225$, [14] the predicted g values for the isotropic doublets are $g_{\Gamma_7} = \frac{17}{3} g_{\text{Landé}} = 7.4942$ and $g_{\Gamma_6} = 5 g_{\text{Landé}} = 6.6125$.

Gd^{3+}

Trivalent gadolinium has a $4f^7$ configuration and a free-ion ground state of $^8S_{7/2}$. The operator-equivalent parameters are zero, and therefore no splitting of the eightfold-degenerate levels by the crystal field is predicted. Experimentally, some of the degeneracy is removed by the interaction with the crystalline electric field; and although the exact nature of the interaction is not understood, the observed spectrum may be fitted to a "spin" Hamiltonian which has the same symmetry as the crystalline electric field. Further, since the splitting is relatively small, seven or more transitions may be observed between the eight energy levels, and the coefficients of the polynomial angular-momentum operators may be determined directly from the EPR spectrum.

EXPERIMENTAL

Single crystals of $KMgF_3$ (mp = 1075 °C) containing up to 3 wt% of the appropriate rare-earth fluoride were grown using the Bridgman method. The starting materials were powders of 99.99%-pure KF (Research Organic/Inorganic Chemical Corp.), >99.99%-pure MgF_2 (prepared and purified from MgO supplied by the Kanto Chemical Co.), and >99.9%-pure LnF_3 (prepared from rare-earth sesquioxides, Ln_2O_3, supplied by the Michigan Chemical Corp.). The fluorides were obtained by slowly heating mixtures of the respective oxides with NH_4HF_2 at temperatures up to 500 °C in a platinum crucible under inert gas atmosphere. Equimolar portions of MgF_2 and KF and 1–3 wt% of LnF_3 were mixed together and inserted into cylindrical platinum ampoules (1.5-cm diam, 8 cm tall, 1-mm wall). The ampoules were heated to 1125 °C under forepump vacuum for outgassing, sealed, and subsequently lowered through 40 cm of negative thermal gradient from 1125 °C to room temperature at a rate of approximately 0.25 cm/h.

The above procedure of slow cooling to room temperature favored formation of regions of crystal inhomogeneity, visually evidenced by optical and density variations in the lower portions of the boule. This problem could usually be eliminated by air-quenching the ampoules from 800 °C, but the thermal shock caused the boules to crack along their {100} cleavage planes. However, the resulting boule fragments always included clear colorless crystals up to 0.5×0.5×0.5 cm. Still larger crystals could be obtained if the ampoule diameter were increased; but the above sizes were more than adequate for our purposes. Emission and mass spectrographic analyses indicated that the dopant impurity content of the crystals approximately equaled the initial doping level for Yb, Er, Dy, and Gd. However, the assayed impurity levels in the crystals containing thulium (70 ppm) and holmium (400 ppm) were decidedly lower than in the initial charge.

The EPR investigations were carried out at X band, using a TE_{011} cylindrical cavity with 2-kHz modulation. ^{60}Co γ rays with a flux of 2.4×10^6 R/h were employed to convert the initially trivalent thulium to divalent thulium. Irradiations were made at either 300 or 77 K and most EPR measurements were made at room temperature, 77, 4.2, and 1.5 K.

Yb^{3+}

Cubic

For crystals of $KMgF_3:Yb^{3+}$, the spectrum shown in Fig. 2(a) was observed at both 4.2 and 1.5 K. The lines indicated by the stick diagram were isotropic with respect to magnetic-field orientation and could be fitted to the spin Hamiltonian

$$\mathcal{H} = g\mu_B \vec{H}\cdot\vec{S} + A\vec{I}\cdot\vec{S} , \qquad (2)$$

where $S=\frac{1}{2}$; $I=0$, $\frac{1}{2}$, or $\frac{5}{2}$; $g = 2.584\pm0.001$; $A_{5/2}(^{173}\text{Yb}) = (188.5\pm0.2)\times10^{-4}$ cm^{-1}; and $A_{1/2}(^{171}\text{Yb}) = (684.7\pm1.0)\times10^{-4}$ cm^{-1}. Their linewidths varied with field orientation and were narrowest when $\vec{H}$ was parallel to a ⟨111⟩ direction. The linewidth of the $^{\text{even}}Yb^{3+}$ line was 20 G in the ⟨111⟩ directions and 25 G in both the ⟨110⟩ and ⟨100⟩ directions. The g value identifies the ground state as belonging to the Γ_6 doublet.

Axial

Two different sets of axial centers were observed. For one, the symmetry axes were the four ⟨111⟩ axes with $g_\parallel = 1.844\pm0.001$ and $g_\perp = 2.896\pm0.002$; for the other, the symmetry axes were the three ⟨100⟩ axes with $g_\parallel = 1.078\pm0.001$ and $g_\perp = 4.377 \pm 0.004$. The hyperfine structure of these centers was too weak to measure. (Only the central line

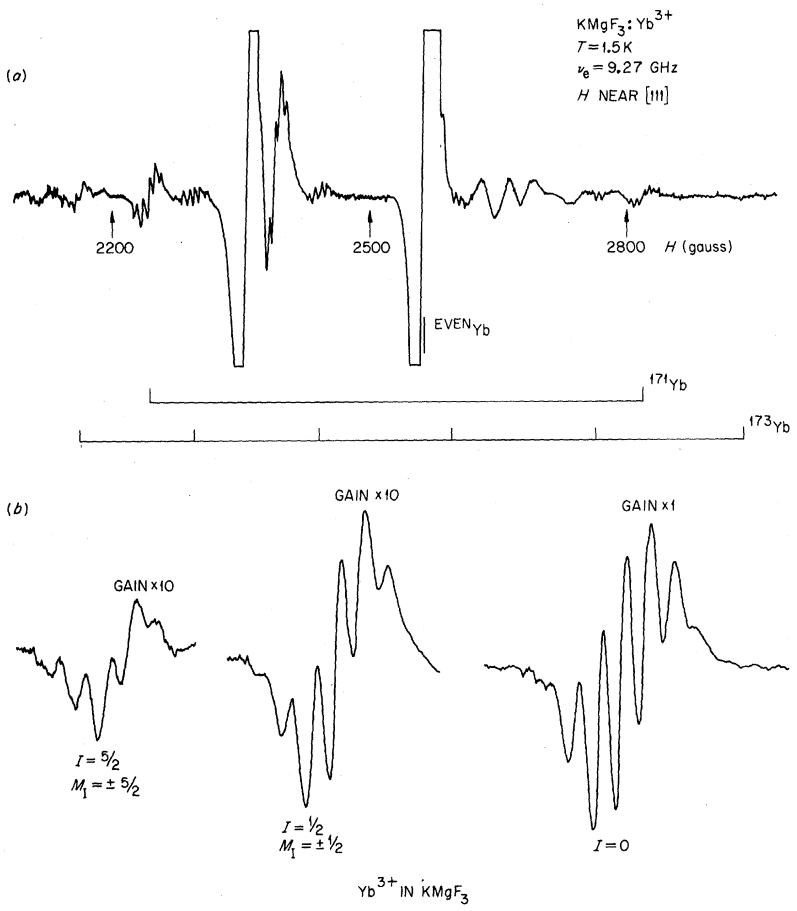

FIG. 2. EPR spectrum of $KMgF_3$: Yb^{3+} for $\vec{H}$ near [111]. (a) Isotropic cubic lines are depicted by the stick diagram below. If $\vec{H}$ were exactly parallel to [111], the large axial lines would be superimposed. (b) Cubic lines with amplification showing superhyperfine lines due to the neighboring fluorines.

due to the even-even isotopes was measured for all the axial centers observed.) The ⟨100⟩ centers were approximately one-half as abundant as the ⟨111⟩ centers and appeared to have longer relaxation times (i.e., saturated more easily). The linewidths for the two axial centers were noticeably different. The ⟨111⟩ axial centers exhibited linewidths varying between 20 and 30 G, while the linewidths for the ⟨100⟩ centers were approximately 10 G.

Superhyperfine Interactions

Figure 2(b) shows some of the cubic lines with higher resolution for $\vec{H}\|[111]$. This clearly shows a superhyperfine interaction with the neighboring ^{19}F ions. There are seven lines indicating an interaction with six equivalent fluorine nuclei. The additional terms

$$\sum_{ij}(\vec{I}_i^F \cdot \vec{A}_{ij}^F \cdot \vec{S}_j - \gamma_n^F \hbar \vec{H} \cdot \vec{I}_i^F)$$

should be added to the spin Hamiltonian with the separation between the lines in this [111] direction approximately equal to 7.2 ± 0.2 G. The structure was only weakly resolved along the [110] direction and was not resolved along the [100], preventing any careful study of the angular variation of the superhyperfine interaction.

The axial centers also exhibited splitting due to ^{19}F. For the ⟨100⟩ centers, the superhyperfine structure was only resolved when $\vec{H}$ was perpendicular to a principal [100] axis with a separation of the order of 4.0 G, while when $\vec{H}$ was parallel to the axis, there was no structure. (Between $\Theta = 0°$ and $\Theta = 10°$, the line was actually split into two lines ~ 38 G apart, showing an additional interaction that was not further investigated.) For the ⟨111⟩ axial centers, superhyperfine structure was resolved when the field was either parallel or perpendicular to a principal [111] axis (splittings were ~ 8.5 and 6.0 G, respectively), but for some intermediate angles, the structure was not resolved. For both types of centers, it was difficult to make a definitive statement concerning the number of fluorine ions involved.

Tm^{2+}

Cubic

In the as-grown crystals of $KMgF_3$ doped with thulium, no spectrum was observed at 4.2 and 1.5 K. The crystals were subsequently irradiated with

γ rays at 77 K, mounted into the EPR spectrometer without an intervening warm-up, and the spectrum due to divalent thulium shown in Fig. 3 was observed at 4.2 K. The two lines were isotropic in position and could be fitted to Eq. (2) with $S=\frac{1}{2}$, $I=\frac{1}{2}$, $g=2.591\pm0.001$, and $A_{1/2}(^{169}\mathrm{Tm})=(283.0\pm1.0)\times10^{-4}$ cm^{-1}. The linewidths varied with field orientation and were ~12 G at their narrowest with $\vec{H}\|\langle111\rangle$. There was no resolution of any superhyperfine structure in any direction. The g value identifies the ground state as a Γ_6 doublet similar to the isoelectronic Yb^{3+}.

It was found that the Tm^{2+} was quite stable, since the spectrum at 4.2 K appeared undiminished following several days storage at room temperature. Divalent thulium could also be produced by a room-temperature irradiation, although not as efficiently. No axial Tm^{2+} spectra were observed in any of the samples.

Er^{3+}

Cubic

For crystals of $KMgF_3:Er^{3+}$, the spectrum shown in Fig. 4 was observed, consisting of a large central line due to the even-even isotopes of erbium and eight hyperfine lines for $^{167}\mathrm{Er}(I=\frac{7}{2})$. The positions of the lines varied with magnetic-field orientation, and with the assumption that $S=\frac{1}{2}$, there were three different g values for the central line: $g_{100}=4.029\pm0.004$, $g_{111}=3.955\pm0.004$, and $g_{110}=3.974\pm0.004$. The hyperfine constant $A_{7/2}(^{167}\mathrm{Er})=(142.8\pm1.0)\times10^{-4}$ cm^{-1} was measured with $\vec{H}\|\langle100\rangle$ only, as the resolution was poorer in the other directions. The g-value variation indicates that this

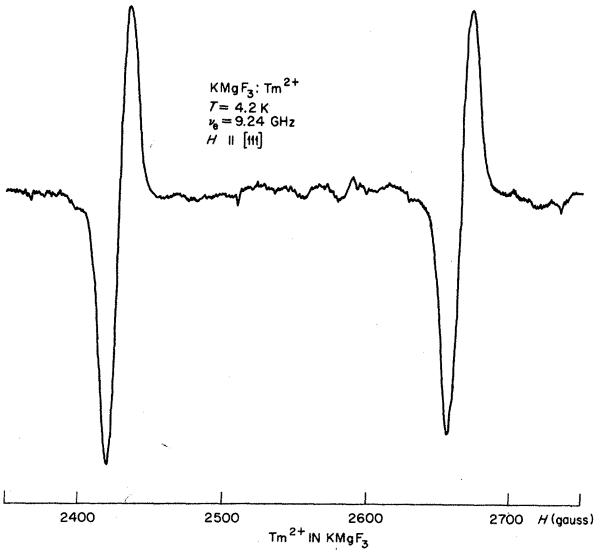

FIG. 3. EPR spectrum of $KMgF_3:Tm^{2+}$ for $\vec{H}\|[111]$. Isotropic cubic lines have narrowest linewidth in this direction.

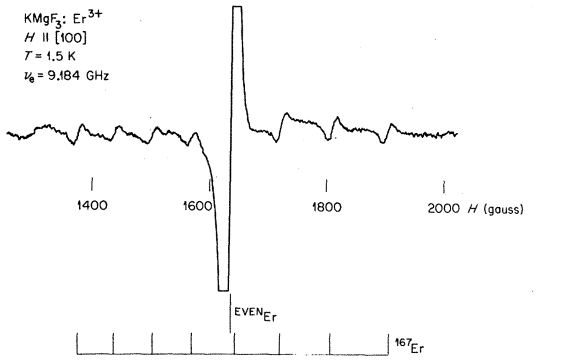

FIG. 4. EPR spectrum of $KMgF_3:Er^{3+}$ for $\vec{H}\|[100]$. Anisotropic cubic lines are depicted by the stick diagram below.

is the $|\frac{1}{2}\rangle \leftrightarrow |-\frac{1}{2}\rangle$ transition of a Γ_8 quartet. With Ayant's[15] notation of $\langle\frac{3}{2}|J_z|\frac{3}{2}\rangle=P$ and $\langle\frac{1}{2}|J_z|\frac{1}{2}\rangle=Q$, then

$$g_{100}=2Qg_{\mathrm{Landé}}', \quad g_{111}=(P-Q)g_{\mathrm{Landé}}',$$

$$g_{110}=\{-\tfrac{1}{2}(P+Q)+\tfrac{1}{2}[7(P^2+Q^2)-2PQ]^{1/2}\}g_{\mathrm{Landé}}'.$$

Fitting the experimental g values to these formulas in the manner outlined by Abraham *et al.*[16] to maintain consistency, we arrive at the values $P=5.044$, $Q=1.7025$, $x=0.678$, and $g_{\mathrm{Landé}}'=1.183$. The linewidth varied slightly with magnetic-field orientation and was about 10 G for the central line.

Axial

Two sets of axial centers were observed whose symmetry axes were the four $\langle111\rangle$ axes. For one center, $g_\parallel=4.216\pm0.004$ and $g_\perp=7.886\pm0.008$, and for the other, $g_\parallel=4.394\pm0.004$ and $g_\perp=7.08\pm0.01$. A third axial center was observed with $\langle100\rangle$ symmetry axes with $g_\parallel=2.682\pm0.005$ and $g_\perp=8.362\pm0.010$.

Superhyperfine Interaction

Figure 5 shows the central cubic line with increased gain for $\vec{H}$ parallel to the three principal directions. The best resolution is clearly with $\vec{H}\|\langle100\rangle$, where the splitting is approximately equal to 3.8 G.

Some dopant segregation occurred during crystal growth, as indicated by a variation in the boule color. The clear boule sections were more lightly doped, and the intensity of the axial spectra was reduced. Only in these clear crystals could the superhyperfine structure be resolved. The pink sections of the boule were more heavily doped (as evidenced by the more intense axial spectra) and no superhyperfine structure could be resolved in specimens from those sections.

Ho^{2+}

No EPR spectrum attributable to holmium was

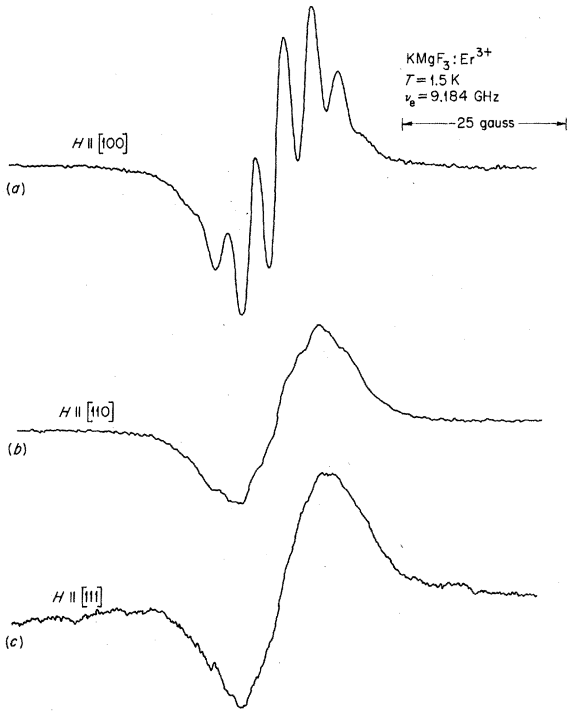

FIG. 5. EPR spectra of cubic central $I=0$ erbium line in $KMgF_3:Er^{3+}$ for $\vec{H}$ parallel to the three principal crystallographic directions.

observed in the as-grown crystals doped with trivalent holmium, or in crystals which were γ irradiated at 77 K. The samples were subjected to a radiation dose of up to 1.5×10^7 R and were mounted in the EPR spectrometer without an intervening warm-up. Searches for a holmium spectrum were unsuccessful at 4.2 and 1.5 K.

Dy^{3+}

Cubic

For crystals of $KMgF_3:Dy^{3+}$, the spectrum shown in Fig. 6(a) was observed at 4.2 and 1.5 K. Only absorption lines which were isotropic with respect to magnetic-field orientation were seen, and these could be fitted to Eq. (2) with $S=\frac{1}{2}$, $I=0$ or $\frac{5}{2}$, $g=6.544\pm0.006$, $A_{5/2}(^{163}\mathrm{Dy})=(274.2\pm1.0)\times10^{-4}$ cm^{-1}, and $A_{5/2}(^{161}\mathrm{Dy})=(194.2\pm1.0)\times10^{-4}$ cm^{-1}. The g value identifies the ground state as belonging to the Γ_6 doublet. Their linewidths varied greatly with field orientation and were narrowest with $\vec{H}\parallel\langle111\rangle$. A linewidth of about 15 G was observed with $\vec{H}\parallel\langle111\rangle$ which broadened to ~35 G with $\vec{H}\parallel\langle100\rangle$.

Superhyperfine Interactions

Figure 6(b) shows the central cubic line under high gain. There is some resolution of structure with $\vec{H}\parallel\langle111\rangle$, but no resolved structure with $\vec{H}\parallel\langle100\rangle$, where the linewidth broadens.

Gd^{3+}

Cubic

The spectrum shown in Fig. 7 was observed for crystals of $KMgF_3:Gd^{3+}$. The intensities and angular variations of the lines are characteristic of an $S=\frac{7}{2}$ state in a cubic crystal field.[17] The crystal field is comparatively weak, and seven $\Delta M_s=\pm1$ transitions may be observed among the eight energy levels. The cubic crystal-field parameters $b_4=60B_4$ and $b_6=1260B_6$ are tabulated in Table II for different temperatures. By studying the relative intensity of the lines between 4.2 and 1.5 K, the sign of b_4 was ascertained to be negative. From this it follows that at zero magnetic field the ordering of the states in energy is a Γ_6 doublet lowest at zero energy, a Γ_8 quartet at $-12b_4+36b_6$, and a Γ_7 doublet highest at $-32b_4+8b_6$. The cubic spectrum was enhanced a factor of 4 by heating the crystal to 1200 K and then quenching in acetone, a procedure which also reduced the extra lines due to lower symmetry sites. Linewidths were approximately 10 G.

Noncubic

An additional Gd^{3+} spectrum was detected whose symmetry has not yet been determined. There were four different sites which were equivalent with $\vec{H}\parallel\langle100\rangle$. Further work will be necessary to determine whether the symmetry is axial or orthorhom-

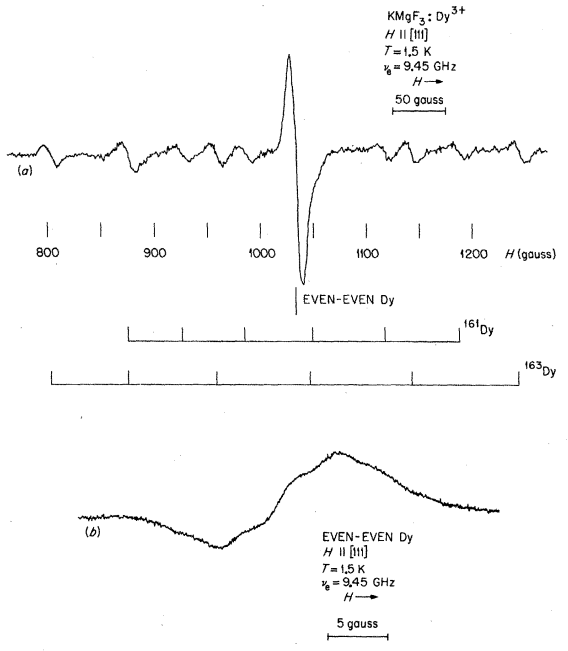

FIG. 6. EPR spectrum of $KMgF_3:Dy^{3+}$. (a) Isotropic cubic lines are depicted by the stick diagram below. (b) The cubic central $I=0$ line for $KMgF_3:Dy^{3+}$ is shown for $\vec{H}\parallel[111]$.

bic. Since the splitting is comparatively large ($b_2^0 \simeq 1200 \times 10^{-4}$ cm^{-1}), the experiments will be done with a higher-frequency EPR spectrometer (35 GHz) in order to determine the spin-Hamiltonian parameters more accurately.

Superhyperfine Interactions

Figure 8 shows the central cubic line under much higher resolution for $\vec{H}$ parallel to the three principal directions. The superhyperfine structure was clearly resolved for $\vec{H} \| \langle 100 \rangle$ and $\langle 110 \rangle$ with little resolved structure for $\vec{H} \| \langle 111 \rangle$. Approximate splittings along the [100] and [110] were 3.3 and 2.5 G, respectively, and it appears that there are more than seven superhyperfine lines in the former case.

DISCUSSION

Experimental results for the observed cubic and axial spectra are summarized in Tables I–III.

For the cubic Yb^{3+} and Tm^{2+} sites, their Γ_6 ground states, plus the fact that their anisotropic EPR linewidths are narrowest with $\vec{H} \| [111]$, imply that they occupy the Mg^{2+} ion site. The Mg site has the required sixfold coordination, and for $\vec{H} \| [111]$ the superhyperfine interactions with the six fluorines located along $\langle 100 \rangle$ directions would all be equivalent. Since fluorine has a spin of $\frac{1}{2}$, this would split the resonance lines into $2\sum_i I_i^F + 1 = 7$ equally spaced

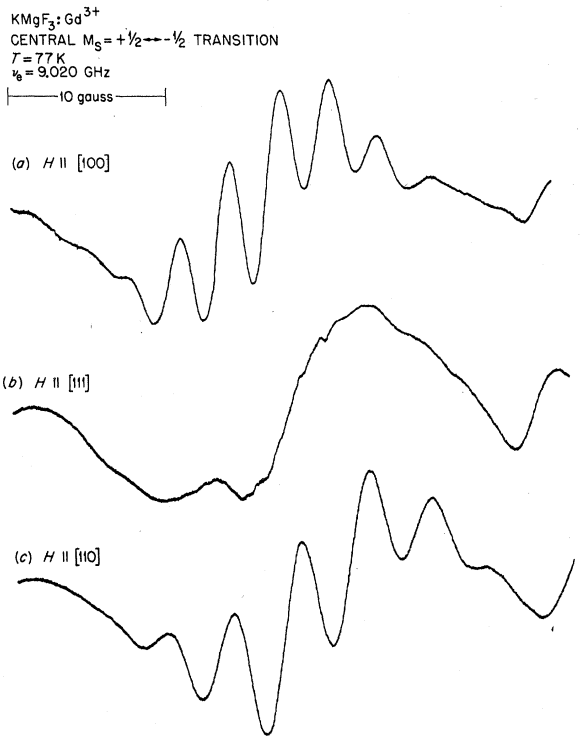

FIG. 8. Cubic central $M_s = \frac{1}{2} \leftrightarrow M_s = -\frac{1}{2}$ line for $KMgF_3$:Gd^{3+} for $\vec{H}$ parallel to the three principal crystallographic directions.

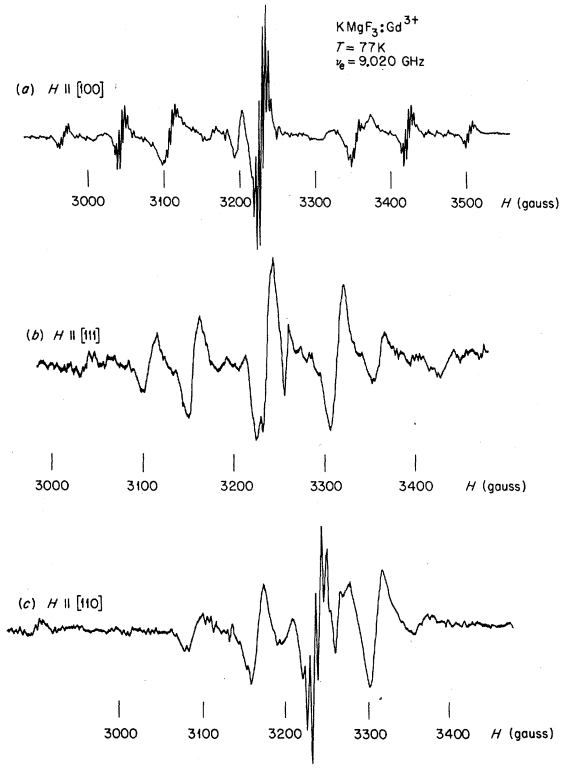

FIG. 7. EPR spectrum of $KMgF_3$:Gd^{3+} for $\vec{H}$ parallel to the three principal crystallographic directions.

superhyperfine components with relative intensities 1:6:15:20:15:6:1. This is seen in Fig. 2(b) for Yb^{3+}. No structure was observed in the Tm^{2+} spectrum.

When the separation between the superhyperfine lines becomes small, the superhyperfine interaction term and the fluorine nuclear Zeeman term become comparable, and hence only an ENDOR experiment can determine unequivocally the relative importance of the two interactions. (In our case, the fluorine

TABLE I. Cubic spectra results for $KMgF_3$:Ln.

Ion	g	Ground state	Site coordination	Hyperfine constant (10^{-4} cm^{-1})
Yb^{3+}	2.584 ± 0.001	Γ_6	6	$^{171}A_{1/2} = 684.7 \pm 1.0$ $^{173}A_{5/2} = 188.5 \pm 0.2$
Tm^{2+}	2.591 ± 0.001	Γ_6	6	$^{169}A_{1/2} = 283.0 \pm 1.0$
Er^{3+}	$g_{100} = 4.029 \pm 0.004$ $g_{111} = 3.955 \pm 0.004$ $g_{110} = 3.974 \pm 0.004$	Γ_8	6	$^{167}A_{7/2} = 142.8 \pm 1.0$ for $\vec{H} \| [100]$
Dy^{3+}	6.544 ± 0.006	Γ_6	6	$^{161}A_{5/2} = 194.2 \pm 1.0$ $^{163}A_{5/2} = 274.2 \pm 1.0$

TABLE II. Cubic spin-Hamiltonian parameters for $KMgF_3:Gd^{3+}$.

Temp (K)	g	$b_4=60B_4$ (10^{-4} cm^{-1})	$b_6=1260B_6$ (10^{-4} cm^{-1})	Total spread[a] (MHz)
297	1.9916±0.0005	−11.15±0.05	+1.20±0.05	1.98
110	•••	•••	•••	2.24
77	1.9916±0.0005	−12.94±0.05	+1.33±0.05	2.29
4.2	1.9916±0.0005	−13.52±0.05	+1.31±0.05	2.39

[a]Distance between outer lines $\frac{7}{2}\leftrightarrow\frac{5}{2}$ and $-\frac{7}{2}\leftrightarrow-\frac{5}{2}$ with $\vec{H}\parallel[100]$ (measured with proton resonance 42.576 MHz $=10^4$G).

nuclear Zeeman term is ~ 2.8 G.) Ranon and Hyde[18] performed this experiment on $CaF_2:Yb^{3+}$, and showed that under this condition the situation can be complicated, since so-called "forbidden" transitions have intensities comparable to the allowed transitions and extra lines may occur. By performing EPR experiments at two different frequencies (and hence changing the value of the nuclear Zeeman term), they were able to explain the superhyperfine structure considering only the eight nearest-neighbor fluorines. The superhyperfine tensor was separated into an isotropic and an anisotropic part and compared with the results of Bessent and Hayes[5] on isoelectronic Tm^{2+} in CaF_2. They concluded that the isotropic term was larger for Tm^{2+} than for Yb^{3+} with the inequality reversed for the anisotropic term. Since in $KMgF_3$ the superhyperfine structure for Tm^{2+} is not resolved, it would appear that the anisotropic portion of the interaction is larger than the isotropic portion, which is similar to the situation in CaF_2. Apparently the electronic wave functions of divalent thulium have less overlap with the fluorine wave functions than do the trivalent ytterbium electronic wave functions. A plausible explanation might be that there is a larger Coulombic force between the trivalent rare-earth ion and the fluorine (which effectively increases the overlap) than between the divalent ion and the fluorine.

The experimental g values for Er^{3+} are only consistent with the ground-state Γ_8 quartet eigenfunctions (given by LLW) which result from sixfold coordination. The resultant value of $x=0.678$ is comparable with those reported for the erbium-doped sixfold-coordinated crystals of MgO ($x=0.72$),[19] CaO ($x=0.732$),[20] and SrO ($x=0.744$).[20] Furthermore, the g values cannot be fitted to the other possible Γ_8 quartet wave functions which would result from twelvefold coordination. Consequently, the superhyperfine structure is expected to be best resolved for $\vec{H}\parallel[111]$, where the six fluorine nearest neighbors are all equivalent. The spectra shown in Fig. 5 are in contradiction to this expectation. In this case, ENDOR measurements are required to define the relative magnitudes of the superhyperfine and nuclear Zeeman interactions.

For Dy^{3+}, the Γ_6 ground state clearly indicates that the impurity is in the sixfold Mg^{2+} lattice site. The linewidth variation due to the superhyperfine lines is also in accord with this identification.

The point-charge model breaks down for the case of S-state ions. Abraham and Boatner[21] have shown that the temperature variation of Gd^{3+} EPR spectra in various cubic crystals appears to depend on the type of cubic coordination. In that work, the *absolute* change in the total spread of the EPR spectrum (for $\vec{H}\parallel[100]$) from 1.5 to about 500 K was the same for the same cubic coordination, regardless of the different crystal-field strengths in the various crystals. It is predominantly the fourth-order term B_4 which varies with temperature, and since the temperature variation of the total spread of the cubic $KMgF_3:Gd^{3+}$ EPR spectrum is similar to that for the eightfold-coordinated fluorite-type crystals and not the sixfold-coordinated alkaline-earth-oxide (NaCl-type) crystals, we conclude that the Gd^{3+} is in the twelvefold K^{1+} site in $KMgF_3$. The superhyperfine lines seen in Fig. 8 do not contradict this conclusion. For this site, there is no magnetic-field direction in which the interactions with all twelve fluorine ions are equivalent. The f-electron orbits contract with increasing atomic number (lanthanide contraction), and presumably the larger trivalent gadolinium goes into the larger potassium site.

Heavier rare-earth doping of the crystals reduced the resolution of superhyperfine lines by broadening the lines and also increased the relative abundance of noncubic to cubic symmetry sites. The latter is, of course, to be expected, since the heavier the doping, the closer the proximity of the required charge-compensating mechanisms which would lower the local symmetry.

It is expected for both Yb^{3+} and Er^{3+} axial spectra caused by small perturbations of the cubic crystal field, and for negative charge compensation, that $g_\parallel<(g\ \text{cubic})<g_\perp$.[22-24] This is the case for all axial spectra in Table III. For small perturbations the average value of $\frac{1}{3}(g_\parallel+2g_\perp)$ is an indication of which cubic ground state is perturbed,[25] and hence which lattice site is probably involved. Initially, several

TABLE III. Axial spectra in $KMgF_3$. (The use of Roman numerals in this paper is only for the purpose of classifying the axial sites).

Ion	$g_\parallel$	$g_\perp$	Average $g=\frac{1}{3}(g_\parallel+2g_\perp)$	Principal axes
Yb^{3+}-I	1.844±0.001	2.896±0.002	2.545	⟨111⟩
Yb^{3+}-II	1.078±0.001	4.377±0.004	3.277	⟨100⟩
Er^{3+}-I	4.216±0.004	7.886±0.008	6.663	⟨111⟩
Er^{3+}-II	4.394±0.004	7.08 ±0.01	6.185	⟨111⟩
Er^{3+}-III	2.682±0.005	8.362±0.010	6.469	⟨100⟩

different cubic ground states may be present due to different x values.

The g values given in Table III indicate that the $\langle 111 \rangle$ and $\langle 100 \rangle$ axial centers of ytterbium arise from an Yb^{3+} ion residing in Mg^{2+} and K^{1+} lattice sites, respectively. The axial symmetry of both spectra may be explained by the same type of charge-compensating mechanism, i.e., missing K^{1+} ions (one for Yb-I and two for Yb-II).

The g values given in Table III for erbium indicate that Er-I and Er-III had lowest Γ_7 cubic ground states before the axial perturbation, and for these spectra the erbium ion probably resides in the sixfold Mg^{2+} site. The Er-II g values indicate that initially a Γ_6 cubic ground state was lowest in energy; therefore, the erbium ion producing this center probably resides in the twelvefold K^{1+} site.

A potassium vacancy could produce the spectra for Er-I, while a substitutional oxygen ion at a fluorine site could produce the Er-III center, and the Er-II center could be produced by a Mg vacancy. These speculations on the nature of the axial sites are plausible, but other interpretations are possible.

For example, a trigonal distortion of the cubic field would split the Γ_8 quartet and create a doublet with the g values [26] $g_{\parallel} = (P - Q)g_{\text{Landé}} = 3.955$ and $g_{\perp} = (P + Q)g_{\text{Landé}} = 7.981$. Both the Er-I and Er-II axial centers have values that do not differ greatly from these, and thus both centers could conceivably be the result of small distortions of the cubic Mg site.

As is usually characteristic of irradiation-produced rare-earth divalency, no spectra were observed that could be associated with Tm^{2+} or Ho^{2+} in noncubic sites. No divalent holmium appeared to be produced by ionizing radiation at 77 K, but divalent thulium could be produced in cubic sites, and was stable at room temperature. This was true even though analyses showed that in these crystals the holmium impurity level (400 ppm) was higher than the thulium impurity level (70 ppm). The amount of thulium and holmium incorporated into the crystals was considerably less than that in the starting melt, which was in contrast to the other rare-earth impurities.

It is concluded from the experimental evidence that rare-earth ions can occupy the sixfold-coordinated Mg site in $KMgF_3$ and still possess cubic symmetry. Rare earths have been observed in the alkaline-earth oxides with sixfold cubic coordination, but due to the high melting points (2000–3000 °C) of these oxides, the crystals are usually grown in an electric arc furnace. This method requires a large and costly amount of rare-earth impurity dopant. The cubic perovskites, on the other hand, with their lower melting points, are ideal hosts for the incorporation of impurities into sixfold-cubic-coordinated sites, and large crystals may be grown. Cubic perovskites with larger lattice constants should also allow the incorporation of the larger ions at the beginning of the rare-earth series.

ACKNOWLEDGMENT

The authors are grateful to R. B. Quincy, who performed the necessary purification of the starting MgF_2 powder.

---

†Research sponsored by the U. S. Atomic Energy Commission under contract with Union Carbide Corp.

*Metals and Ceramics Division, Oak Ridge National Laboratory, Oak Ridge, Tenn.

‡Oak Ridge Graduate Fellow from the University of Tennessee under appointment from the Oak Ridge Associated Universities.

[1]M. T. Hutchings, in *Solid State Physics*, edited by F. Seitz and D. Turnbull (Academic, New York, 1964), Vol. XVI, p. 277; B. Bleaney, Proc. Roy. Soc. (London) A277, 289 (1964); W. Low and E. L. Offenbacher, in *Solid State Physics*, edited by F. Seitz and D. Turnbull (Academic, New York, 1965), Vol. XVII, p. 135.

[2]R. W. G. Wyckoff, *Crystal Structures* (Wiley, New York, 1964), Vol. II, p. 390.

[3]J. M. Baker, W. Hayes, and M. C. M. O'Brien, Proc. Roy. Soc. (London) A254, 273 (1960).

[4]B. G. Berulava and T. I. Sanadze, reported by S. A. Al'tshuler and B. M. Kozyrev, *Electron Paramagnetic Resonance* (Academic, New York, 1964), p. 132.

[5]R. G. Bessent and W. Hayes, Proc. Roy. Soc. (London) A285, 430 (1965).

[6]W. Low and U. Ranon, in *Proceedings of the First International Conference on Paramagnetic Resonance, Jerusalem*, edited by W. Low (Academic, New York, 1963), Vol. I, p. 167; U. Ranon and J. S. Hyde, Phys. Rev. 141, 259 (1966).

[7]C. M. Bowden, Bull. Am. Phys. Soc. 11, 834 (1966); Ph. D. thesis (Clemson University, 1967) (unpublished); C. M. Bowden and J. E. Miller, J. Phys. Chem. Solids 30, 1661 (1969).

[8]K. W. H. Stevens, Proc. Phys. Soc. (London) A65, 209 (1952); B. Bleaney and K. W. H. Stevens, Rept. Progr. Phys. 16, 108 (1953).

[9]M. T. Hutchings, in *Solid State Physics*, edited by F. Seitz and D. Turnbull (Academic, New York, 1964), Vol. XVI, p. 227.

[10]K. R. Lea, M. J. M. Leask, and W. P. Wolf, J. Phys. Chem. Solids 23, 1381 (1962).

[11]A. Y. Cabezas and I. P. K. Lindgren, Phys. Rev. 120, 920 (1960).

[12]B. Bleaney, Proc. Phys. Soc. (London) B73, 939 (1959).

[13]L. S. Goodman, H. Kopfermann, and K. Schlüpmann, Naturwiss. 49, 1 (1962).

[14]S. Penselin and K. Schlüpmann, quoted by B. R. Judd and I. Lindgren, Phys. Rev. 122, 1802 (1961).

[15]Y. Ayant, in *Proceedings of the First International Conference on Paramagnetic Resonance, Jerusalem*, edited by W. Low (Academic, New York, 1963), Vol. I, p. 267; Y. Ayant, E. Belorizky, and J. Rosset, J. Phys. Radium 23, 201 (1962).

[16]M. M. Abraham, C. B. Finch, L. J. Raubenheimer, Z. M. el Saffar, and R. A. Weeks, in *Proceedings of the Fourteenth Colloque Ampère: Magnetic Resonance and Relaxation, Ljubljana*, 1966 (North-Holland, Amsterdam, 1967), p. 282.

[17]See, for example, M. M. Abraham, L. A. Boatner, C. B. Finch, E. J. Lee, and R. A. Weeks, J. Phys. Chem. Solids 28, 81 (1967).

[18]U. Ranon and J. S. Hyde, Phys. Rev. 141, 259 (1966).

[19]D. Descamps and Y. Merle d'Aubigne, Phys. Letters 8, 5 (1964).

[20]I. C. Chang and W. W. Anderson, Phys. Letters 13, 112 (1964).

[21]M. M. Abraham and L. A. Boatner, J. Chem. Phys. 51, 3134 (1969).

[22]U. Ranon and W. Low, Phys. Rev. 132, 1609 (1963).

[23]M. M. Abraham, R. A. Weeks, G. W. Clark, and C. B. Finch, Phys. Rev. 137, A138 (1965).

[24]M. M. Abraham, R. A. Weeks, G. W. Clark, and C. B. Finch, Phys. Rev. 148, 350 (1966).

[25]H. R. Lewis and E. S. Sabisky, Phys. Rev. 130, 1370 (1963).

[26]A. Abragam and B. Bleaney, *Electron Paramagnetic Resonance of Transition Ions* (Clarendon, Oxford, England, 1970), p. 730.

PHYSICAL REVIEW B VOLUME 3, NUMBER 9 1 MAY 1971

Electron-Paramagnetic-Resonance Investigations of $5f^5$ Configuration Ions in Cubic Single Crystals: Pu^{3+} in ThO_2 and $SrCl_2$, and Am^{4+} in ThO_2 †

M. M. Abraham, L. A. Boatner, * C. B. Finch, ‡ and R. W. Reynolds *
Solid State Division, Oak Ridge National Laboratory, Oak Ridge, Tennessee 37830
(Received 18 December 1970)

Electron-paramagnetic-resonance spectra of the isoelectronic ions Pu^{3+} and Am^{4+} in cubic sites of fluorite-structure single crystals have been investigated at 1.5 and 4.2 K. The observed isotropic spectra and associated g values identify the ground states as Γ_7 doublets. This ground state is produced by intermediate-coupling effects which are much larger for $5f^5$ configuration ions than for the analogous $4f^5$ ions. Spin-Hamiltonian parameters were determined to be: $g = 1.3124 \pm 0.0005$, $A = (65.4 \pm 0.2) \times 10^{-4}$ cm^{-1} for $^{239}Pu^{3+}$ in ThO_2; $g = 1.1208 \pm 0.0005$, $A = (127.9 \pm 0.4) \times 10^{-4}$ cm^{-1} for $^{239}Pu^{3+}$ in $SrCl_2$; and $g = 1.2862 \pm 0.0005$, $A = (45.7 \pm 0.1) \times 10^{-4}$ cm^{-1} for $^{241}Am^{4+}$ and $A = (45.3 \pm 0.1) \times 10^{-4}$ cm^{-1} for $^{243}Am^{4+}$ in ThO_2. Spectra observed for both Pu^{3+} and Am^{4+} were characterized by very anisotropic linewidths and by a dependence of linewidth on the nuclear-spin projection quantum number m_I.

I. INTRODUCTION

Although the electronic properties of $5f^n$ (actinide) ions are somewhat similar to those of the corresponding $4f^n$ (rare-earth) ions, some important differences occur as a result of intermediate-coupling effects. An illustration of the significance of intermediate coupling for the actinide ions was provided by a comparison[1] of wave functions calculated for the $J = \frac{5}{2}$ ground-state term of Sm^{3+} ($4f^5$) and Pu^{3+} ($5f^5$). For pure Russell-Saunders coupling, the Hund's-rule ground state for an f^5 configuration is $^6H_{5/2}$. A comparison of the intermediate-coupled wave functions, however, indicated that although the ^6H term contributes 96% to the ground state of Sm^{3+}, it contributes only 66% to the Pu^{3+} ground state.

The large admixture of higher-lying $J = \frac{5}{2}$ states changes the predicted splitting by a cubic crystal field of the Pu^{3+} ground-state term. A calculation of the fourth-order crystal-field operator-equivalent factors $\langle \Psi_J || \beta || \Psi_J \rangle$ has been carried out by Edelstein *et al.*[1] using intermediate-coupled wave functions for Sm^{3+} and Pu^{3+}. From this calculation they found that intermediate coupling resulted in a difference in the sign of the factor $\langle \Psi_J || \beta || \Psi_J \rangle$ for Pu^{3+} relative to that obtained for Sm^{3+} (or for a pure $^6H_{5/2}$ state). For Sm^{3+} and Pu^{3+} in an eightfold-coordinated cubic site, this difference in sign determines that the Γ_8 quartet lies lowest for Sm^{3+}, while the Γ_7 doublet lies lowest for Pu^{3+}. Experimentally, Edelstein *et al.*[1] have verified that the Γ_7 doublet is the ground state for Pu^{3+} in CaF_2, SrF_2, and BaF_2. Their measured g values for Pu^{3+} were different in each host due to varying crystal-field-produced admixtures of the Γ_7 doublet in the first excited $J = \frac{7}{2}$ state. A Γ_8 ground state for Sm^{3+} in an eightfold-coordinated cubic site has not been reported, although axial spectra have been observed[2,3] in CaF_2.

An interpretation of the Pu^{3+} hyperfine parameters as measured in three fluorite-structure hosts has been given recently by Edelstein and Mehlhorn.[4] Intermediate-coupling effects were again important, and the varying admixture of the excited Γ_7 doublet also resulted in significant variations in the magnitude of the hyperfine parameter which corresponded to observed effects.

We report here the observation of Pu^{3+} EPR spectra in the fluorite-structure single crystals ThO_2